Nanoscale Advances

ROYAL SOCIETY OF CHEMISTRY

PAPER

View Article Online
View Journal | View Issue

Cite this: *Nanoscale Adv.*, 2022, **4**, 1999

Reversible conjugation of biomembrane vesicles with magnetic nanoparticles using a self-assembled nanogel interface: single particle analysis using imaging flow cytometry†

Ryosuke Mizuta,[a] Yoshihiro Sasaki, *[a] Kiyofumi Katagiri, [b] Shin-ichi Sawada[a] and Kazunari Akiyoshi*[a]

Nanoscale biomembrane vesicles such as liposomes and extracellular vesicles are promising materials for therapeutic delivery applications. However, modification processes that disrupt the biomembrane affect the performance of these systems. Non-covalent functionalization approaches that are facile and easily reversed by environmental triggers are therefore being widely investigated. In this study, liposomes were successfully hybridized with magnetic iron oxide particles using a cholesterol-modified pullulan nanogel interface. Both the magnetic nanoparticles and the hydrophobic core of the lipid bilayer interacted with the hydrophobic cholesteryl moieties, resulting in stable hybrids after simple mixing. Single particle analysis by imaging flow cytometry showed that the hybrid particles interacted in solution. Calcein loaded liposomes were not disrupted by the hybridization, showing that conjugation did not affect membrane stability. The hybrids could be magnetically separated and showed significantly enhanced uptake by HeLa cells when a magnetic field was applied. Differential scanning calorimetry revealed that the hybridization mechanism involved hydrophobic cholesteryl inserting into the biomembrane. Furthermore, exposure of the hybrids to fetal bovine serum proteins reversed the hybridization in a concentration dependent manner, indicating that the interaction was both reversible and controllable. This is the first example of reversible inorganic material conjugation with a biomembrane that has been confirmed by single particle analysis. Both the magnetic nanogel/liposome hybrids and the imaging flow cytometry analysis method have the potential to significantly contribute to therapeutic delivery and nanomaterial development.

Received 25th November 2021
Accepted 13th March 2022

DOI: 10.1039/d1na00834j

rsc.li/nanoscale-advances

Introduction

Biomembrane-based supramolecular assemblies have recently attracted attention in the field of advanced medicine. In particular, extracellular vesicles (EVs), including exosomes, are of increasing interest in the biomedical field because they play important roles in various biological phenomena such as immune response and signal transduction as an intercellular communication medium.[1] EV is a general term for vesicles delimited by biological membranes that are released by almost all cells.[2] It has been shown that membrane proteins and glycolipids exist on the surface layer of EVs, and various proteins and nucleic acids including DNA and RNA exist inside them.[3] Due to their constituent elements, EVs have been shown to exhibit features such as low immunogenicity and excellent biocompatibility, thus making them promising nanocarriers for drug delivery system (DDS) and therapeutic agents.[4–6] To apply EVs to DDS, it is desirable that EVs are efficiently delivered to target tissues and cells. For this purpose, biomembrane engineering has recently been applied to develop methods of hybridizing various materials into EVs.[7] Biomembrane engineering continues to attract the interest of researchers in the biomedical field because of its potential in the development of new therapeutics.[8] Reported approaches have enabled the functionalization of biomembranes with bioactive molecules,[9] ligands for targeting,[10] and particles for drug loading,[11] to control functions and impart new properties. The application of biomembrane engineering to cells have been widely studied for cell surface engineering for the development of cell-based therapies.[12,13]

On these ground, we focused on the targeted delivery of biomembrane vesicles by hybridization with magnetic microparticles. Since the strength and direction of the magnetic field can be easily controlled, it has attracted attention in the field of drug delivery as a method for targeting specific sites and

[a]*Department of Polymer Chemistry, Graduate School of Engineering, A3-317, Kyoto University, Katsura, Nishikyo-ku, Kyoto 615-8510, Japan. E-mail: akiyoshi@bio.polym.kyoto-u.ac.jp; Fax: +81-75-383-2590; Tel: +81-75-383-2823*

[b]*Department of Applied Chemistry, Graduate School of Engineering, Hiroshima University, 1-4-1 Kagamiyama, Higashi-Hiroshima, 739-8527, Japan*

† Electronic supplementary information (ESI) available. See DOI: 10.1039/d1na00834j

improving delivery efficiency.[14] There have been reports on the efficient delivery of various drugs such as small molecules,[15] nucleic acids,[16] and proteins[17] using magnetic nanoparticles. However, there have not been many examples of delivery methods for supramolecular assemblies with biomembrane structures by magnetic induction. In addition, most of the methods are based on irreversible hybridization of biomembrane vesicles and magnetic nanoparticles.[18]

When delivering biomembrane vesicles by conjugation with magnetic nanoparticles, it is desirable to detach the nanovesicle cargo in the target cells to avoid potential adverse biological effects caused by the nanocarriers. It is therefore necessary to control the conjugation reversibility. However, to the best of our knowledge, no conjugation strategy focusing on such functionality has been established. Controlling the reversibility of conjugation is expected to lead to the development of on-demand, dose-controlled, repetitive drug delivery systems. Modification of EVs by physical conjugation is one effective approach to achieve the reversible conjugation described above. There have been a number of reports of physical conjugation to cell membranes.[19–23] In recent years, there have been several studies applying these methods for modifying cell membranes to EV modification. For instance, there have been various reports of functionalizing EVs by inserting lipid-mimicking compounds with alkyl chains attached to functional molecules, into membranes through hydrophobic interactions.[24,25] The functional modification of EVs using physical conjugation can be expected add new functions while maintaining the excellent biocompatibility of natural biological membrane vesicles.[26] In addition, we have proposed EV hybridization methods with amphiphilic nanogels—functional polymeric nanocarriers.[27] We also applied this method to hybridize EVs with magnetoresponsive carriers. We previously reported the hybridization of EVs with functional inorganic particles by using nanogels formed by the self-assembly of cholesterol-bearing pullulan (CHP)—pullulan partially grafted with cholesteryl groups—as an interface between EVs and inorganic materials.[28] We found that magnetic nanogels containing iron oxide nanoparticles encapsulated in CHP nanogels efficiently hybridized with EVs without affecting the activity of the EVs. This approach can be regarded as a new method for supramolecular chemical conjugation of inorganic materials and biomembrane vesicles using nanogels.

In this study, we investigate the detailed mechanism of the conjugation of iron oxide nanoparticles with nanosized biomembrane vesicles using CHP nanogel as an interface. We used liposomes as a model for nanosized vesicles with a biomembrane structure and evaluated their complexation behavior with magnetic nanogels. In addition, we developed a system to reversibly control the conjugation of magnetic particles to liposomes using nanogels, and extended this system to the EV system. It has been suggested that the interaction between the lipid bilayer and the nanogel is the driving force for the hybridization of biomembranes and CHP nanogels. It has been reported that CHP nanogels formed supramolecular assemblies with giant liposomes consisting of POPC—which have a simpler composition than biomembranes.[29] We have also succeeded in constructing liposome-encapsulating gel materials using liposomes consisting of DMPC coated with reactive nanogels as building blocks.[30] However, the detailed mechanism of the hybridization of the nanogel and the nanosized biomembrane vesicles remains unclear. Elucidation of the mechanism of nanogel hybridization with biomembranes is important for establishing a completely new nanogel-based supramolecular chemical method for biomembrane vesicle conjugation.

It is important to clarify the conjugation mechanism of liposomes with a nanogel interface, not only as a model system, but also for the development of new liposome-based DDS carriers with smart functions. Liposomes are nanovesicles comprising lipid bilayers that can encapsulate both hydrophobic and hydrophilic drugs owing to the hydrophobic areas within the lipid bilayers and an internal aqueous phase, and have been studied as drug carriers for many years.[31] Liposomal drugs have been approved for the treatment of various diseases such as cancer, infectious diseases, and age-related macular degeneration.[32] The modification of liposomes using biomembrane engineering methods has led to the development of therapeutic agents with enhanced properties. Such methods are therefore extremely important in the field of nanomedicine and are actively studied worldwide.[33] Non-genetic engineering approaches are considered highly appropriate for the functionalization of liposomes because they do not use biological processes. For example, it has been reported that cationic liposomes decorated with CpG oligodeoxynucleotides conjugated with antigenic proteins by electrostatic interactions,[34] and amphiphilic peptides conjugated with alkyl chains and cilengitide *via* peptides cleaved by enzymes highly expressed in tumor endothelial cells, can be inserted into the liposome surface by hydrophobic interactions.[35]

Based on this background, we propose an approach to liposome modification: reversible non-covalent conjugation of functional nanocarriers loaded with inorganic particles. This is the first report of reversible conjugation of inorganic materials and biomolecular assemblies by hydrophobic interaction using a hydrophobic polysaccharide as an interface. This functionalization approach is based on hybridizing lipid membranes and inorganic nanoparticles *via* the intermolecular forces between them and a nanogel. In this study, we found that the cholesteryl group of the nanogel was inserted into the biomembrane, resulting in the hybridization of the liposome and magnetic nanogel. In addition, we report a new imaging flow cytometry method for confirming the hybridization of nanoparticles at the single particle level. This new application of the analytical technique allows us to analyze the heterogeneity of synthetic nanoparticles on a single particle level, which has previously been difficult. It was also found that the reversal of nanogel conjugation was controllable.

Results and discussion

Hybridization of magnetic nanogels and liposomes

We investigated the hybridization of nanosized biomembrane vesicles and iron oxide nanoparticles using CHP nanogel as an interface (Fig. 1A). It has been suggested that CHP nanogel can

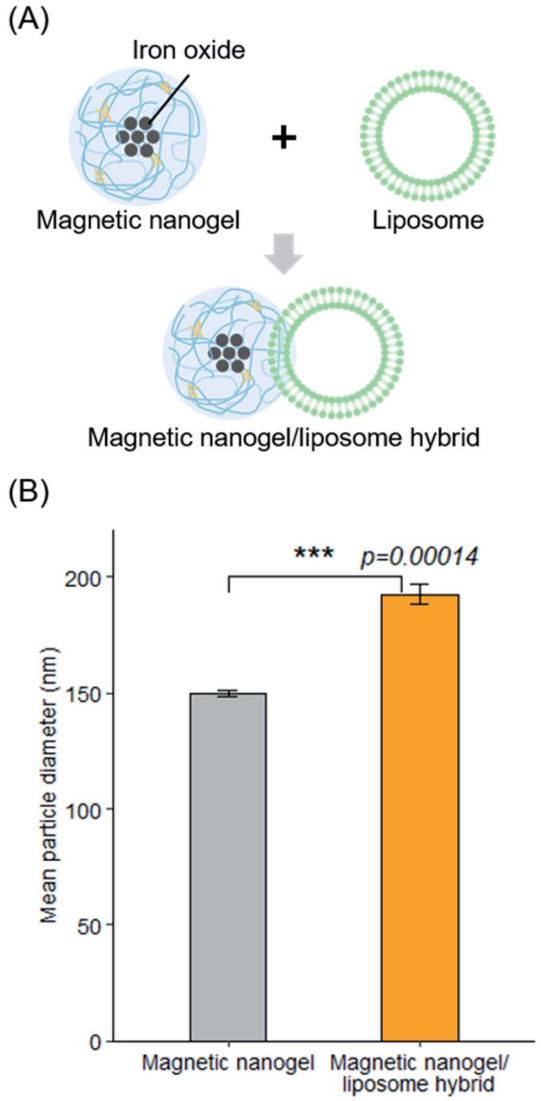

Fig. 1 Hybridization of magnetic nanogels and liposomes. (A) Schematic illustration of the preparation of magnetic nanogel/liposome hybrids. (B) Particle size distribution of magnetic nanogels and magnetic nanogel/liposome hybrids. Statistical comparison was made between the magnetic nanogels and hybrids. The experiments were carried out in triplicate ($n = 3$) and data are presented as mean ± s.d. Statistical analysis was conducted using Welch's t test. ***$p \leq 0.001$.

be complexed with giant liposomes. We therefore assumed that the nanogel and lipid bilayer also interact in the hybridization of magnetic nanogels and biomembrane vesicles such as EVs. Thus, we used liposomes made from a thin lipid film consisting of DOPC as a biomembrane vesicle model. Dynamic light scattering measurements showed that the average particle size of the prepared liposomes was 108 nm, with a polydispersity index of 0.09. Magnetic nanogels were prepared using a modified version of a previously reported method.[36] Specifically, iron oxide nanoparticles coated with hydrophobic groups were added to a self-assembled nanogel dispersion consisting of cholesteryl group-substituted pullulan with a particle diameter of approximately 30 nm, using a syringe pump. The added iron oxide nanoparticles complexed with the nanogels *via* hydrophobic interactions to form magnetic nanogels. The average particle size of the obtained magnetic nanogel was 150 nm with a polydispersity index of 0.17 (Fig. S1†).

The effectiveness of hybridization by simple mixing of the two particles was investigated first. After mixing the particle size distribution had clearly changed, and the average particle size was 182 nm with a polydispersity index of 0.15 (Fig. 1B). This suggests that the magnetic nanogels and liposomes could be combined by simple mixing. When we mixed the magnetic nanogels with liposomes of various particle size using the same approach, the particle size of the prepared hybrids increased with increasing size of the liposomes used for the hybridization (Fig. S2†). This indicated that the method can be used to functionalize liposomes with magnetic nanogels regardless of their particle size. In addition, the dependence of the hybrid size on the liposome introduced, suggests that the liposome retained its structure while the hybridization took place.

Single particle analysis of the liposome and magnetic nanogel hybridization

We aimed to evaluate the interaction and hybridization of the magnetic nanogels and liposomes at the single particle level. To date, it has been difficult to quantitatively evaluate the interaction between such nanoparticles, except by applying relatively challenging techniques. In addition, methods to statistically analyze the interactions of particles in solution at the single-particle level remain under development. Such techniques can reveal the composition of nanoparticles dispersed in solution and can be very important indicators for estimating the efficiency of nanoparticle functionalization and the properties of the prepared particles. Therefore, we focused on imaging flow cytometry. Imaging flow cytometry provides the throughput and statistical analysis of a flow cytometer and the imaging capability of a fluorescence microscope and can detect the fluorescence and scattered light of nanoparticles in a flow path. Previously, imaging flow cytometry has been used to reveal the heterogeneity of nanoparticles in extracellular vesicles[37,38] and liposomes[39] based on their fluorescence. In this study, we applied these techniques to the analysis of synthetic nanoparticles including magnetic nanogels and liposome–magnetic nanogel hybrids.

Prior to analyzing the hybrids, we studied the magnetic nanogels and liposomes used for hybrid preparation. For the liposome analysis gating, we distinguished the nanoparticles of the sample from the speed beads for flow control based on the intensity of the side scatter and the area of the bright field image, and only gated particles were analyzed. We then plotted the results against the fluorescence of the NBD and the side scatter and determined that the population with the highest density of particles detected was the sample, while particles with side scatter that was too high were considered to be aggregates or artifacts and were removed (Fig. S3†). To calibrate the device, the size standard beads were measured using above gating set up (Fig. S4†). As a result, it was confirmed that the beads could be distinguished and detected according to their size and associated particle fluorescence. It has been shown

that there were clusters of iron oxide nanoparticles in the magnetic nanogels and it was assumed that the clusters increased the lateral scattering intensity.[40] Therefore, for the magnetic nanogels, we separated the sample from the speed beads as described, and then analyzed the particles with no NBD fluorescence and high SSC intensity. As a result, populations with a particular distribution were confirmed for both particles (Fig. S5†). To confirm that the particles detected by the instrument were not contaminating particles, but particles derived from the sample, only the buffer was measured under the same conditions (Fig. S6A†). As a result, almost no particles could be detected in the buffer, suggesting that the particles detected were magnetic nanogels. In addition, when the magnetic nanogel dispersion was serially diluted and the particle concentration was plotted after 3 minutes of measurement, a clear correlation was confirmed (Fig. S6B†). From this result, it was concluded that magnetic nanogels could be analyzed as single particles using imaging flow cytometry. We confirmed the single particle analysis of liposomes consisting of lipid membranes containing NBD–PE in the same way (Fig. S7†). The concentration of particles was clearly higher than that of buffer or unstained liposomes, indicating that fluorescent particles could indeed be detected. When a surfactant was added to the liposomes used, the particle concentration was clearly lowered, confirming that particles with lipid membranes could be detected. Furthermore, an almost linear correlation was observed between the dilution rate and the particle concentration when serially diluted liposomal suspension was measured. Thus, it was concluded that NBD-containing liposomes can be analyzed as single particles.

The spread in the scatter plot obtained from the analysis is considered to represent the distribution of particle size and fluorescence modification. The distribution of liposomes was clearly narrower than that of the magnetic nanogels. This may reflect the narrower distribution of the particle size and the efficiency of fluorescence modification in a single particle. This trend was consistent with the difference in the polydispersity indices of the two types of particle by DLS. The results showed that the prepared nanoparticles exhibited different scattered light and fluorescence profiles, and the gating used allowed separate detection of each particle. In addition, the images of each particle showed bright spots according to the fluorescence and scattered light intensity (Fig. S8†). Therefore, the established gating was used in all measurements of the NBD–PE-containing liposome and magnetic nanogel hybrids.

Next, we analyzed the liposome and magnetic nanogel hybrids. Specifically, we gated for selection a population containing magnetic nanogels and hybrids except for free liposomes. Analysis of this population revealed the ratio of magnetic nanogels hybridized with liposomes. It was found that the distribution of the magnetic nanogel clearly changed as the final concentration of the mixed liposomes increased (Fig. 2A–C). At liposome concentrations of 0.01 and 0.1 mM, most of the particles were detected in the same position as the magnetic nanogel and were not fully hybridized. For magnetic nanogels mixed with liposomes at a final lipid concentration of 1 mM, approximately 98% of the particles in the region where the fluorescence intensity of NBD was similar to that of liposomes had the same scattering light intensity as that of nanogels (denoted "Hybrid" in the scatter plot). This indicated that the distribution of the magnetic nanogel shifted owing to hybridization with the liposomes. These results showed that magnetic nanogels interacted with liposomes at the single particle level. The fluorescence images of the particles detected in the hybrid gating showed that the single particles exhibited scattered light similar to that of magnetic nanogels and co-localized bright spots of liposome-derived fluorescence and the fluorescence of the rhodamine-modified nanogels (Fig. 2D). Such particles were not observed when the component particles were analyzed alone. This indicates that the liposome and magnetic nanogel hybrids could be successfully analyzed at the single particle level.

Because the analysis method used can distinguish and detect particles in solution, it is expected to be able to reveal the distribution of nanoparticles dispersed in solution. Changing the number of liposomes added to the magnetic nanogels was found to change the ratio of magnetic nanogels to hybrids (Fig. S9†). This finding indicated that the percentage of nanoparticles detected in the magnetic nanogel region decreased as the number of liposomes increased, and the distribution shifted toward the hybrid gate. Plotting the ratio of the hybrid against the liposome concentration showed that the addition of 1 mM liposome to 100 μg mL^{-1} magnetic nanogel was sufficient for hybridization (Fig. 2E).

Single-particle analysis of the EV-magnetic nanogel hybrid was also attempted using imaging flow cytometry. The EVs were fluorescently labeled with Exosparkler green, and the magnetic nanogels were conjugated with rhodamine. A 60× lens was used for the measurements, and 488 nm and 560 nm lasers were used at maximum power. The size standard beads were measured first (Fig. S10†). It was confirmed that each bead could be detected separately by particle size and fluorescence intensity. Based on these results, the particles were gated. Specifically, bright-field observation revealed gated regions with only nanoparticles without artifacts (Fig. S11A†). Using this gating, gating was applied based on the fluorescence of each particle (EV, exosparkler green; magnetic nanogel, rhodamine; Fig. S11B and C†). Then, each particle was measured using the gating (Fig. S12†). In addition, we measured a variety of control samples to check whether single particle analysis was possible (Fig. S13 and S14†). As for EVs, the number of particles was significantly reduced in the unstained and surfactant-added samples, as was the case for liposomes, confirming that single particle analysis of EVs was indeed possible. Furthermore, when each particle was serially diluted, there was a correlation between the dilution rate and the number of particles.

Magnetic nanogels and EVs were mixed to final concentrations of 100 μg mL^{-1} and 50 μg mL^{-1} (protein concentration), respectively, and the prepared hybrids were analyzed (Fig. 2F). Single particle analysis was performed focusing on the EVs in the dispersion. As a result, the distribution of EVs was clearly changed and the fluorescence derived from magnetic nanogel was confirmed from single EVs. The results showed that the biomembrane vesicles and iron oxide nanoparticles were hybridized using the nanogel as an interface, similar to the

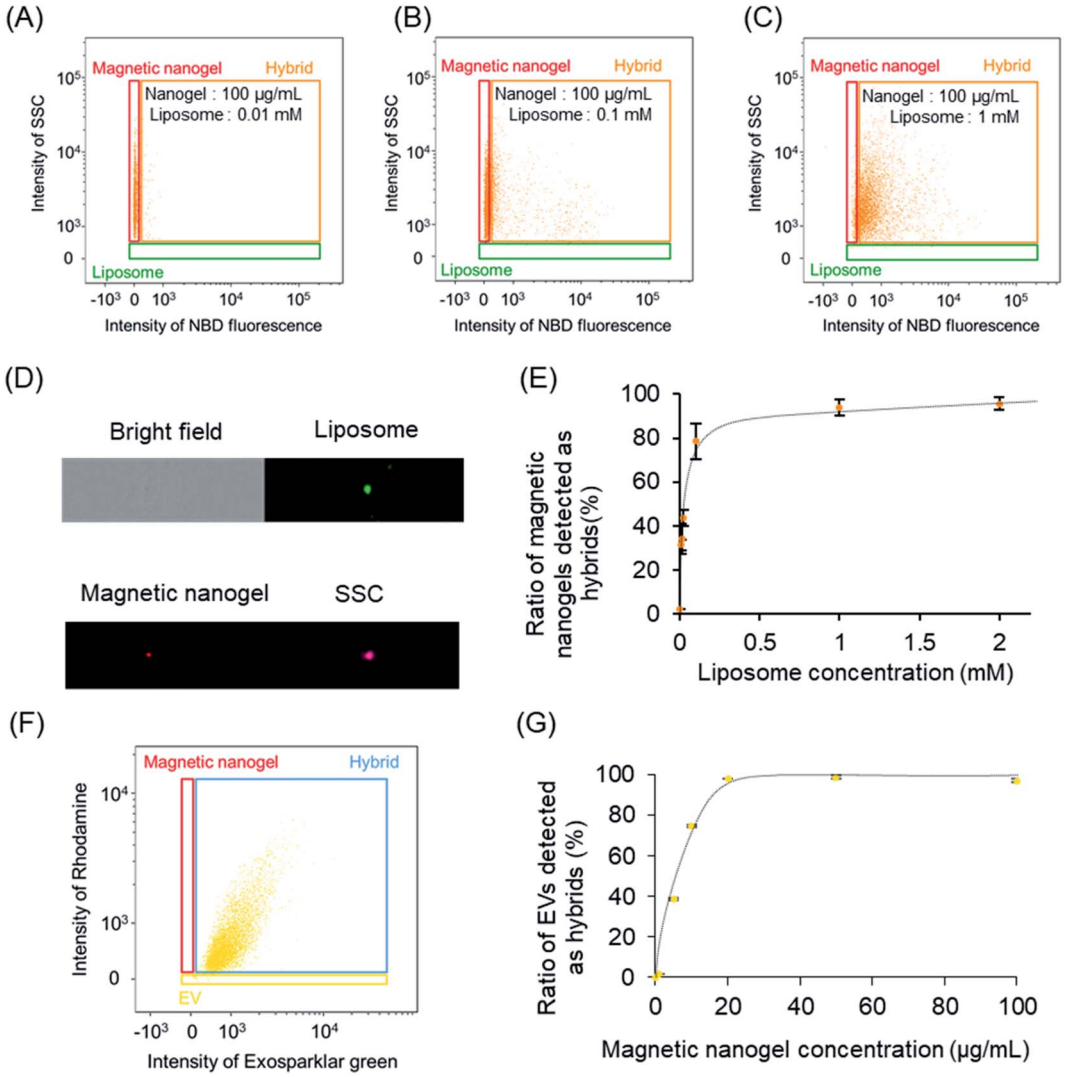

Fig. 2 Single particle analysis of the hybrids using imaging flow cytometry. In the analysis, the particles detected in the gating region of the magnetic nanogel were analyzed. For samples containing EVs, stained EVs were measured and their distribution were shown. (A) Distribution of particles in a magnetic nanogel and liposome mixture at final concentrations of 100 μg mL^{-1} and 0.01 mM, respectively. (B) Distribution of particles in a magnetic nanogel and liposome mixture at final concentrations of 100 μg mL^{-1} and 0.1 mM, respectively. (C) Distribution of particles in a magnetic nanogel and liposome mixture at final concentrations of 100 μg mL^{-1} and 1 mM, respectively. (D) Bright-field, fluorescence, and side-scatter images of particles detected in the region of the hybrid. In liposomes, the fluorescence of NBDs in lipid membranes was shown. In magnetic nanogels, fluorescence of rhodamine modified on the polymer was observed. NBD was excited by a 488 nm laser and detected in channel 2. Rhodamine was excited at 488 nm and detected in channel 3. SSC was detected in channel 6. (E) Ratio of hybrids to total magnetic nanogel at each liposome concentration (the plotted values represent the mean and standard deviation of three independent runs). (F) Single particle analysis of magnetic nanogel/EV hybrids using imaging flow cytometry. Distribution changes of particles detected as EVs when magnetic nanogels of 100 μg mL^{-1} were mixed with EVs of 50 μg mL^{-1} final protein concentration. (G) Ratio of hybrids to total EVs at each magnetic nanogel concentration.

liposome as a model system. In addition, when the final concentration of EVs was kept constant and mixed with a series of concentrations of magnetic nanogels, the profile of EVs changed according to the concentration change of magnetic nanogels. It was also found that the ratio of EVs detected as hybrid increased with the increase in the concentration of the added magnetic nanogel (Fig. S15†). This allowed us to analyze the saturation behavior of the hybridization by mixing some high concentration of magnetic nanogel and EV without any separation operation (Fig. 2G). Furthermore, when the fluorescence intensity of the nanogel in a single EV was calculated, the fluorescence was higher than that of a single magnetic nanogel when the amount of added magnetic nanogel exceeded 250 μg mL^{-1} (Fig. S16†). This suggests that more than two particles of magnetic nanogel are hybridized with individual EV. The hybridization between the nanogel and EVs was confirmed by *in situ* imaging flow cytometry without separating the soft biomembrane vesicles from the nanogel.

The imaging flow cytometry analysis method was found to be suitable for evaluating the efficiency of nanoparticle

functionalization because it can reveal the distribution of nanoparticles based on their fluorescence and scattered light. The magnetic nanogel used in this study is a dynamic gel particle stabilized by physical cross-linking, and the liposome is also a relatively soft nanoparticle. Repeated separation and purification operations, using centrifugal force or magnetic force, on the hybrids consisting of such nanoparticles induced morphological changes such as aggregation, making it difficult to evaluate interactions between them in solution. Such manipulations can be minimized using imaging flow cytometry. Therefore, this method is suitable for revealing the composition of soft nanoparticles in solution while minimizing the effects on the particle structure.

Microscopy observation of binding between the magnetic nanogel and lipid bilayer

The functionalization of liposomes with magnetic nanogel is believed to be achieved by interaction between the lipid bilayer and magnetic nanogel. Therefore, we attempted to evaluate the interaction between the magnetic nanogel and lipid bilayer by microscopy observation. Silica particles with a diameter of 10 μm and liposomes with an approximate diameter of 50 nm fluorescently labeled with NBD–PE were mixed by inversion to form lipid bilayer-coated silica particles. The lipid bilayer-coated silica particles were then mixed with rhodamine-labeled magnetic nanogels (Fig. 3A). Confocal laser microscopy showed that the magnetic nanogel fluorescence was only observed when the silica particles were coated with a lipid bilayer (Fig. 3B). This result indicates that there is an interaction between the lipid bilayer and the magnetic nanogel. For a representative particle in each microscopy image, the fluorescence of the nanogel was co-localized with the fluorescence profile of its cross-section only if the particle was also covered by the lipid bilayer (Fig. S17†). Therefore, the two co-localized fluorescence signals are not due to leakage from each other, but rather indicate the hybridization of the magnetic nanogel on the lipid bilayer. These results indicate that interaction between the magnetic nanogel and lipid

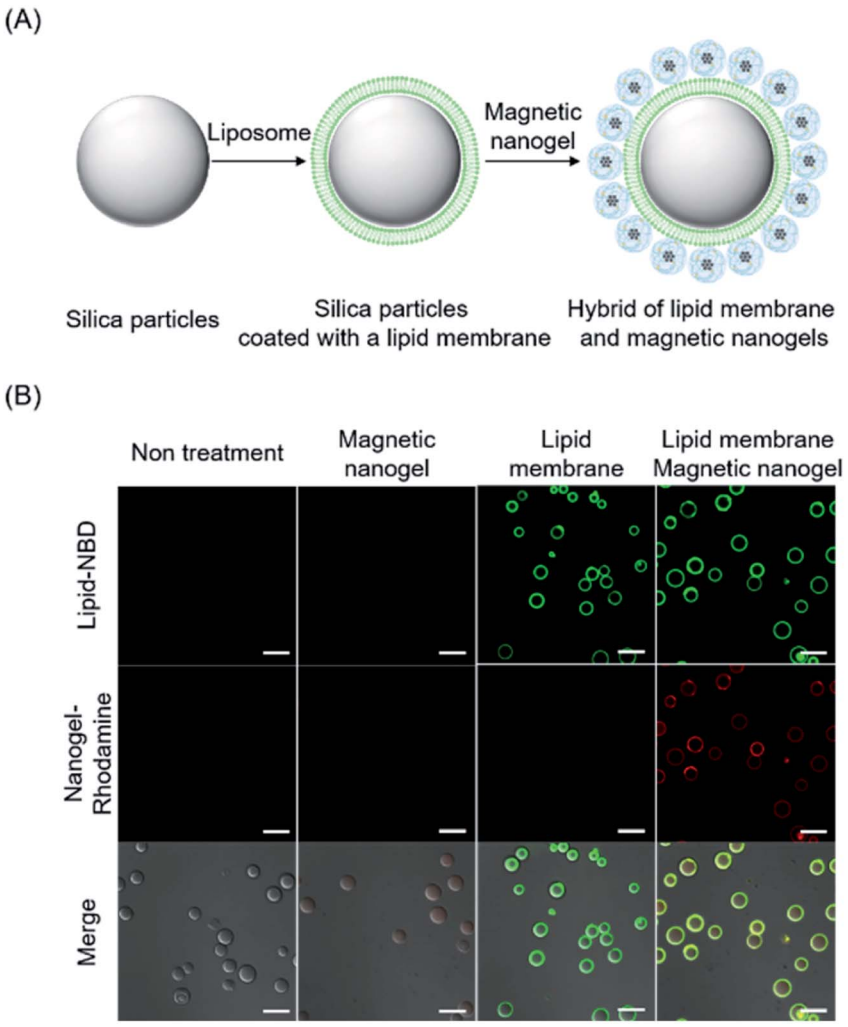

Fig. 3 Microscopy observation of binding between magnetic nanogels and lipid bilayers. (A) Schematic illustration of the preparation of silica particles coated with lipid bilayers and the evaluation of the interaction between the lipid bilayers and magnetic nanogels using silica particles. (B) Evaluation of hybridization between magnetic nanogels and lipid bilayers by confocal laser microscopy. "Lipid membrane" indicates the use of silica particles coated with a lipid bilayer, and "Magnetic nanogel" indicates the addition of magnetic nanogel.

membrane could be the main driving force for the hybridization in the modification of the biomembrane with magnetic nanogel. This behavior was similar to that of CHP nanogels complexed with giant liposomes, suggesting that CHP molecules in magnetic nanogels interact with the lipid bilayers of biomembranes, resulting in stable hybridization.

Interaction of nanogels with membranes

The interaction of the magnetic nanogels with the lipid bilayers was found to be the driving force for the hybridization. In this section, we investigate in greater detail the hybridization mechanism between the magnetic nanogel and lipid bilayer using liposomes as a model. The findings are expected to provide insight into the functionalization mechanism of vesicles with membrane structures of biological origin—including extracellular vesicles—by magnetic nanogels.

The hybridization mechanism was evaluated from differences in lipid membrane fluidity by measuring the change in the endothermic peak of the lipid bilayer using differential scanning calorimetry (DSC) (Fig. 4A). Liposomes containing DMPC were used as a model for nanosized biomembrane vesicles. A peak at the phase transition temperature of DMPC was observed for the liposomes before hybridization. We then measured liposomes mixed with magnetic nanogels and found that the endothermic peak became less pronounced and the phase transition temperature decreased, even though the lipid content was the same. This indicated that the fluidity of the lipid bilayer was increased by hybridization of the magnetic nanogels and liposomes. This behavior is very similar to that of cholesterol added to monolayer liposomes composed of DMPC.[41] This suggests that cholesteryl groups grafted onto pullulan are inserted into the lipid bilayer (Fig. 4B). Therefore, it was found that iron oxide nanoparticles with hydrophobic surface modification and CHP nanogel and biomembranes and CHP nanogel are mutually hybridized by non-covalent intermolecular forces including hydrophobic interactions. This hybridization method is therefore a highly versatile and novel functionalization technique that can be used to conjugate any kind of inorganic particles and biomembrane vesicles. In addition to liposomes, previous studies have reported hybrids using EVs as biological membrane vesicles. In the case of hybridization with EVs, the insertion of the cholesteryl group of the magnetic nanogel into the EV membrane, as clarified herein, is thought to contribute to the hybridization.

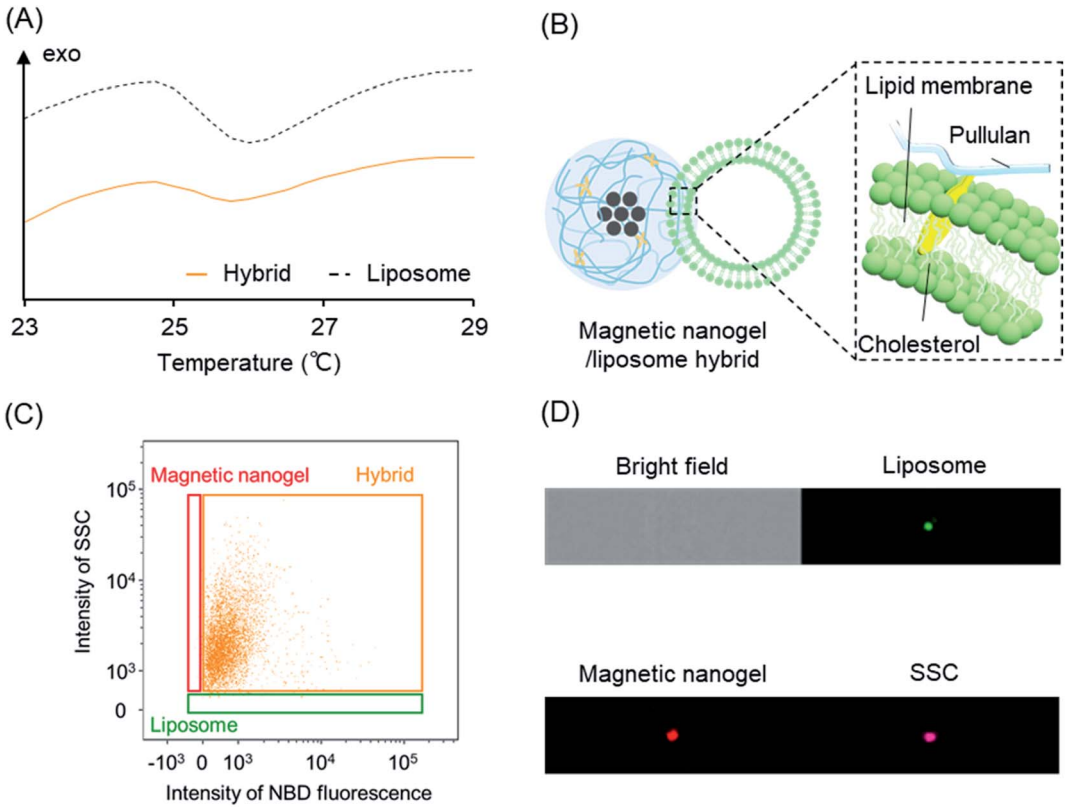

Fig. 4 Evaluation of the interaction of magnetic nanogels and liposomes. (A) Confirmation of hybridization indicated by changes in the endothermic peaks of the lipid bilayers. The dashed line shows the DSC measurement of liposomes made of DMPC, and the solid line shows the DSC measurement of the liposome and magnetic nanogel hybrid. The temperature was varied at a rate of 5 K min^{-1}. The results are shown for the second temperature increase process. (B) Schematic illustration of magnetic nanogels and liposomes hybridized by the insertion of cholesteryl groups. (C) Single particle analysis of hybrids composed of magnetic nanogel and anionic liposomes using imaging flow cytometry. Distribution of particles in magnetic nanogel and liposome at final concentrations of 100 μg mL^{-1} and 1 mM, respectively. (D) Fluorescence image of particles detected in the region of the hybrid.

Next, we investigated the effect of surface charge on the hybridization with magnetic nanogels using cationic and anionic liposomes. The ζ potential of the liposomes was measured to confirm the hybridization. The ζ potentials of cationic liposomes and magnetic nanogels were 34.9 mV and −1.6 mV, respectively. In contrast, the ζ potential of the prepared hybrid was 5.2 mV (Fig. S18A†). This result suggests that the hybridization of cationic liposomes and magnetic nanogels relaxes the surface charge of the liposome. The charge on the liposome surface was also found to be relaxed in the hybridization of anionic liposomes and magnetic nanogels (Fig. S18B†). Specifically, the charge of the liposomes changed from −40.4 mV to −6.76 mV following inversion mixing with magnetic nanogels. This result suggested that anionic liposomes could be hybridized with magnetic nanogel.

Therefore, we performed single particle analysis using imaging flow cytometry on hybrids of cationic and anionic liposomes and magnetic nanogels (Fig. S19,† and 4C and D). The results showed that the liposome-derived fluorescence co-localized with magnetic nanogel even at the single particle level. This indicates that the magnetic nanogel and the biomembrane hybridize regardless of their surface charges. It is known that the membranes of biological membrane vesicles such as exosomes are rich in anionic lipids such as phosphatidylserine.[42] The result that magnetic nanogels can be combined with anionic liposomes suggests that the nanogel-based conjugation system has an excellent feature that it can be implemented for biomembrane vesicles such as exosomes.

Evaluation of the morphology and retention of the internal aqueous phase of liposomes in the hybrids

The retention of vesicular inclusions is very important if functionalized biomembrane vesicles are to be used in drug delivery. In addition, when functionalizing EVs such as exosomes, it is essential to preserve the structure of the vesicles and minimize the impact on their contents.

We evaluated the effect of liposome functionalization with magnetic nanogel on the morphology and internal aqueous phase of liposomes using transmission electron microscopy (Fig. 5A). Observation of the hybrids showed that liposomes consisting of lipid bilayers and magnetic nanogels were hybridized in a conjoined morphology. The particles that made up the hybrids maintained the morphology of the particles used in the preparation (Fig. S20†). This suggests that during magnetic nanogel hybridization, the liposome retains its structure and hybridizes with the nanogel by non-covalent bonding.

Next, liposomes with a lipid membrane of only DOPC and loaded with calcein were prepared and functionalized with magnetic nanogels as previously described. We confirmed that single particle analysis could be also performed for calcein-loaded liposomes (Fig. S21†). The number of particles in the liposome dispersion solution was clearly higher than the particle concentration in the respective control sample, confirming that the particles detected were liposomes. In addition, only the same amount of particles could be detected in the calcein solution as in the buffer, indicating that the sample was able to detect the inner water layer. The prepared hybrids were analyzed using imaging flow cytometry (Fig. 5B). The profiles of the magnetic nanogels changed and the calcein fluorescence derived from the liposome cargo was observed for most of the magnetic nanogels. The distribution of calcein fluorescence per single particle detected in the hybrids was comparable to that of the liposomes used (Fig. S22†). In addition, single particle analysis was carried out for magnetic nanogels mixed with the same amount of calcein as encapsulated in the liposomes (Fig. 5C). No calcein fluorescence was observed for the magnetic nanogel in solution, and the distribution was similar to that of

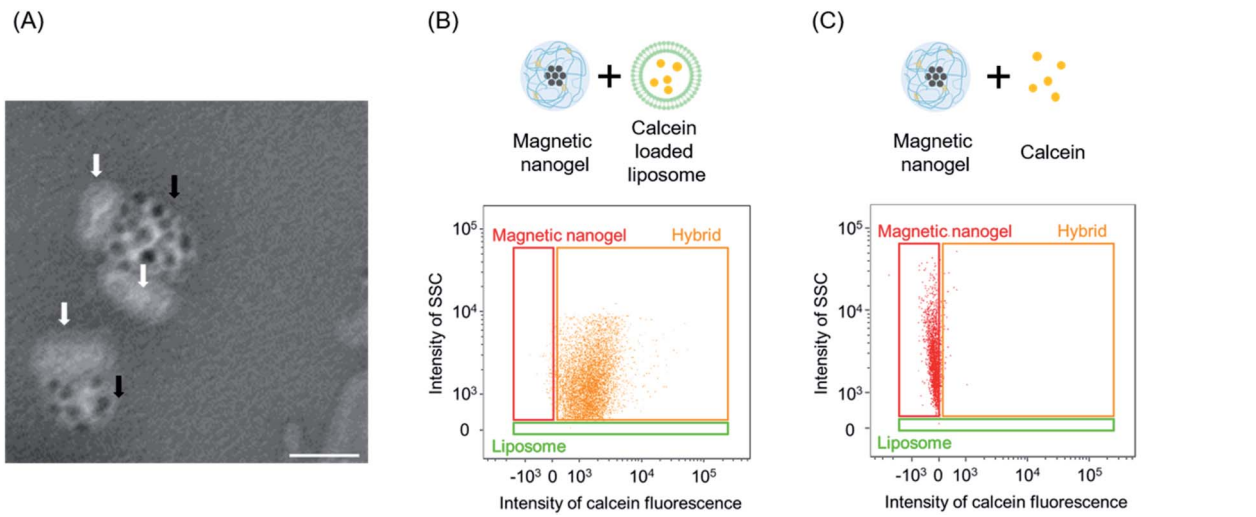

Fig. 5 Structural evaluation of magnetic nanogel/liposome hybrids. (A) TEM image of magnetic nanogel/liposome hybrid. The black arrows indicate magnetic nanogels, and the white arrows indicate liposomes. Scale bar represents 100 nm. (B) Single particle analysis of magnetic nanogel and calcein-loaded liposome hybrids by imaging flow cytometry. (C) Single particle analysis of magnetic nanogel mixed with calcein by imaging flow cytometry.

the magnetic nanogel before mixing. These observations suggest that the liposome inclusions were retained on hybridization with the magnetic nanogel. This also suggested that the imaging flow cytometry analysis method could be applied to inclusions such as fluorescent substances encapsulated in nanoparticles. Furthermore, when surfactant was added to hybrids collected by magnetic separation, 98% of the calcein was released into the supernatant. This observation suggested that calcein was encapsulated in the liposomes hybridized with the magnetic nanogel. When the magnetically separated hybrids were redispersed in buffer and a magnetic field was applied to the solution, 94% of the calcein present in the solution was collected. This indicates that the separated hybrids could be magnetically induced with minimal effect on the inner aqueous phase.

The nanogel-based liposome modification method is therefore thought to be an effective and facile method for functional modification of pre-conditioned liposomes. The findings for these model systems suggest that the functionalization of biomembrane vesicles using magnetic nanogels preserves the structure of the vesicles and retains their cargo. Thus, the nanogel interface strategy is expected to minimize the impact on the structure and inclusions when functionalizing biomembrane vesicles with various cargo.

Magnetically driven intracellular delivery of liposomes

We have achieved the modification of liposomes with magnetic iron oxide nanoparticles while maintaining the structure and inclusions of the liposomes by using a nanogel as an interface between the inorganic particles and biomembrane vesicles. The liposome and magnetic nanogel hybrid is therefore appropriate for application as a liposome delivery system using a magnetic field. We investigated the magnetically driven delivery of liposomes by adding hybrids prepared with fluorescently labeled liposomes to HeLa cells and subsequently applying a magnetic field (Fig. 6A).

The hybrids consisting of liposomes with fluorescently labeled lipid bilayers and magnetic nanogel were added to cells. A magnetic field was then applied to the cells for 1 h with a neodymium magnet, and the intracellular lipid membrane-derived fluorescence was measured by flow cytometry (Fig. 6B). The application of a magnetic field to the hybrids clearly increased the intensity of intracellular lipid membrane-derived fluorescence compared with the cases where no field was applied or only liposomes of the same concentration were added. This indicates that the liposomes were efficiently taken up into the target cells when a magnetic field was applied to the hybrids. Next, hybrids of calcein loaded liposomes and magnetic nanogel were added to the cells, and magnetic induction delivery was carried out for 1 h. Subsequent flow cytometry measurements revealed that the intracellular calcein fluorescence was markedly stronger when a magnetic field was applied (Fig. 6C). This shows that applying a magnetic field to the liposome and magnetic nanogel hybrids led to efficient liposome cargo delivery. These two results indicate that magnetically induced delivery of magnetic nanogel/liposome hybrids can deliver both membranes and encapsulated cargo. These results suggested that this approach could be a versatile method for efficient delivery of artificial membrane vesicles, such as liposome preparations, and natural membrane nanoparticles, including exosomes.

Control of the interaction between magnetic nanogels and liposomes

It has been shown that magnetic nanogels can be hybridized with biomembranes through non-covalent hydrophobic interaction of cholesteryl groups. In addition, previous studies have shown that nanogels and magnetic nanogels can efficiently internalize proteins through hydrophobic interactions with cholesteryl groups.[17] Therefore, we anticipated that by exposing the magnetic nanogel and liposome hybrids prepared herein to high protein concentrations, the magnetic nanogel would complex with the protein and the cholesteryl groups in the nanogel would interact with the protein, separating the hybrids into magnetic nanogels and liposomes. The hybrid of liposomes fluorescently labeled with NBD and magnetic nanogels was exposed to a high concentration of protein and then magnetically separated. By measuring the fluorescence of the supernatant, the ratio of liposomes released from the magnetic nanogels was calculated (Fig. 7A). It was found that increasing the FBS concentration increased the percentage of liposomes in the supernatant. This could indicate that the liposomes were

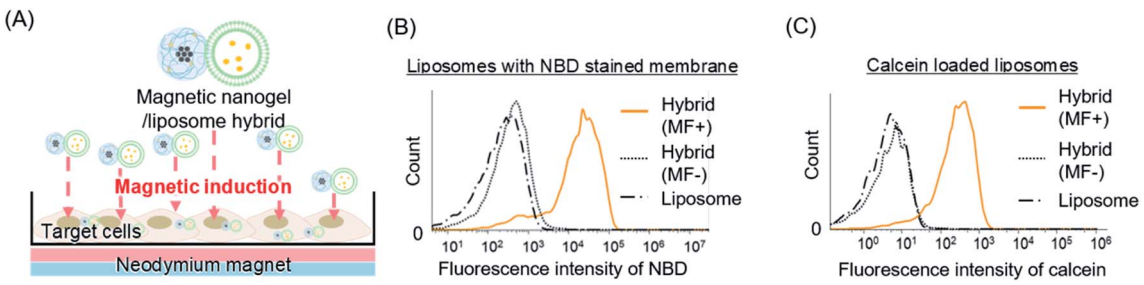

Fig. 6 Evaluation of intracellular delivery efficiency of liposome delivery system using a magnetic field. (A) Schematic illustration of intracellular delivery of liposomes by decoration with magnetic nanogel. (B) Evaluation of intracellular delivery of liposomes with lipid membrane fluorescently labeled with NBD, using flow cytometry. (C) Evaluation of intracellular delivery of liposome inclusions by flow cytometry using calcein loaded liposomes. MF represents the magnetic field.

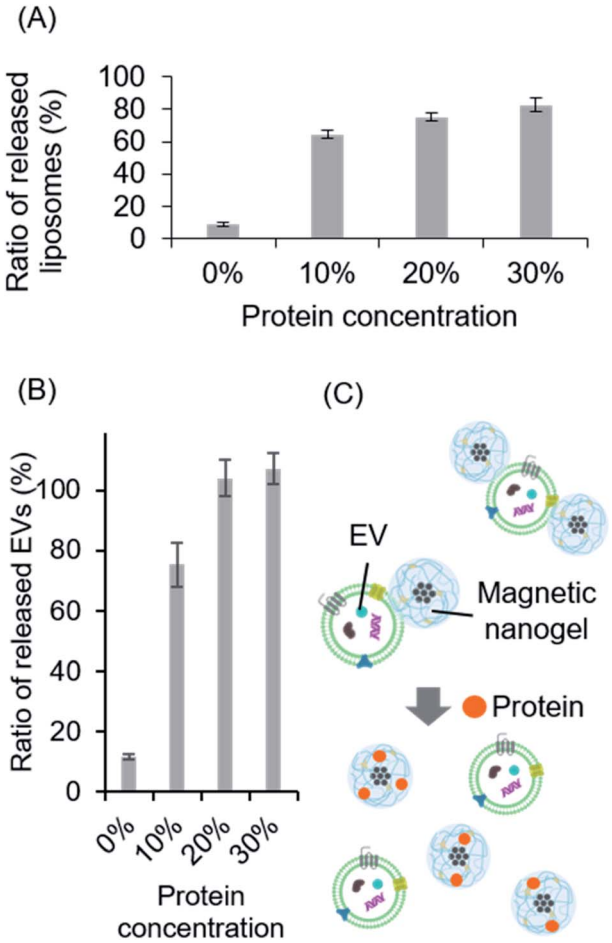

Fig. 7 Controlled release of hybridized magnetic particles and biomembrane vesicles using a nanogel interface. (A) Ratio of liposomes released from the hybrids in the presence of different concentrations of FBS. (B) Ratio of EVs released from the magnetic nanogels in the presence of different concentrations of FBS. (C) Schematic illustration of the switching of biomembrane vesicle functionalization using magnetic nanogels triggered by the presence of proteins.

separated from the magnetic nanogels in the presence of a high concentration of protein. This is thought to be because the cholesteryl groups in the nanogels interacted with the protein when it was encapsulated, and the number of cholesteryl groups available for hybridization with the liposome decreased.

In this case, the liposomes may have detached during the separation process as a result of the application of a magnetic field to hybrids destabilized by the addition of protein. Therefore, we used imaging flow cytometry to directly evaluate the hybrids in solution when the protein was added (Fig. S23†). The number of magnetic nanogels detected as hybrids decreased as the concentration of FBS increased. Furthermore, as the protein concentration increased, the distribution of almost all of the hybrids clearly changed. This indicated that the addition of the protein did indeed separate the liposomes from the hybrids in solution. These results suggested that the functionalization of liposomes with iron oxide nanoparticles using a nanogel interface could allow control of any subsequent separation of the modification. Therefore, we believe that our functionalization method offers a completely new approach for biomembrane functionalization using switchable non-covalent bonds.

The hybrids of magnetic nanogels and vesicles consisting only of lipid molecules were found to be separable in the presence of high concentrations of protein. We evaluated whether this switching of functionalization was also possible in biomembrane vesicles by applying it in a system comprising hybrids of EVs and magnetic nanogels. Specifically, hybrids of fluorescently labeled EVs and magnetic nanogels were exposed to various concentrations of FBS. A magnetic field was then applied to separate the magnetic particles, and the EVs separated from the magnetic nanogel were quantified by measuring the fluorescence of the supernatant. The ratio of EVs separated from the magnetic nanogel to the total number of EVs used for hybridization increased in the presence of high concentrations of protein, as was observed for liposomes (Fig. 7B). Therefore, the functionalization of biomembranes with magnetic nanogels is considered a smart modification method allowing controlled separation in the presence of proteins (Fig. 7C). Furthermore, the functionalization with magnetic nanogel can provide magnetic induction properties to EVs in solution, and is expected to be applied as a new extracellular vesicle separation technology, where the EVs can be separated using a magnetic field and then uncomplexed. Since this methodology allows biomembrane vesicles to be complexed with magnetic nanogels by intermolecular forces, such as hydrophobic interactions, without the use of specific interactions, it is expected to be applied to a broad range of technologies without specific bias to extracellular vesicles. In other words, the technique can collect entire EVs rather than a specific population of extracellular vesicles.

Conclusion

We clarified the hybridization mechanism of inorganic nanoparticles and biomembrane vesicles interfaced with nanogels, using liposomes as a model. We developed a new method for the functionalization of liposomes where the cholesteryl groups of magnetic nanogels are inserted into lipid bilayers *via* hydrophobic interactions, resulting in non-covalent hybridization. This functionalization method endows liposomes with magnetic induction properties through the simple process of inversion mixing of liposomes and magnetic nanogels. In a series of hybridization evaluations, we adapted the imaging flow cytometry analysis method to synthetic nanoparticles as a new way to confirm the hybridization of the two particles. This analysis method provides information that, to date, has been difficult to determine, namely the distribution of synthetic nanoparticles in solution. It also has the potential to reveal the composition of nanoparticles at the single particle level based on fluorescence and scattered light. The present approach, in which liposomes and iron oxide nanoparticles are hybridized through nanogels by intermolecular forces, is a highly versatile method that can be used for hybridization regardless of the type of liposomes or inorganic particles because it does not use any

specific binding. The application of this method to various materials will lead to the development of new DDS carriers that integrate liposome-based carriers and inorganic particles with unique functions. The liposome-based system is a model for exosomes and other extracellular vesicles with biomembrane structures, and it is thought that the cholesteryl group of the magnetic nanogel also inserts into the biomembrane of extracellular vesicles to form hybrids. This hybridization mechanism is expected to contribute significantly to the retention of function in the hybridization of biomembrane vesicles and their inclusions. Furthermore, the functionalization of biomembrane vesicles using a nanogel interface was found to be reversible. There have been few examples of synthetic polymer-mediated conjugation of biomembrane vesicles with inorganic materials where the reversibility of the conjugation has been demonstrated at the single particle level. Therefore, this smart functionalization method is expected to be applied to new techniques for the introduction of biomembrane vesicles into cells and separation methods for extracellular vesicle delivery.

Conflicts of interest

There are no conflicts of interest to declare.

Acknowledgements

This work was supported by a Grant-in-Aid from the Japan Society for the Promotion of Science (JSPS) KAKENHI Grant Number JP16H06313 (K. A.), JP16H03842 (Y. S.), and 21J13562 (R. M.). This work was also supported by a grant from JST CREST Grant Number JPMJCR17H2. We thank Sarah Dodds, PhD, from Edanz (https://jp.edanz.com/ac) for editing a draft of this manuscript and helping to draft the abstract.

References

1 R. Kalluri and V. S. LeBleu, *Science*, 2020, **367**, 640.
2 A. E. Russell, A. Sneider, K. W. Witwer, P. Bergese, S. N. Bhattacharyya, A. Cocks, E. Cocucci, U. Erdbrügger, J. M. Falcon-Perez, D. W. Freeman, T. M. Gallagher, S. Hu, Y. Huang, S. M. Jay, S. Kano, G. Lavieu, A. Leszczynska, A. M. Llorente, Q. Lu, V. Mahairaki, D. C. Muth, N. N. Hooten, M. Ostrowski, I. Prada, S. Sahoo, T. H. Schøyen, L. Sheng, D. Tesch, G. Van Niel, R. E. Vandenbroucke, F. J. Verweij, A. V. Villar, M. Wauben, A. M. Wehman, H. Yin, D. R. F. Carter and P. Vader, *J. Extracell. Vesicles*, 2019, **8**, 1684862.
3 C. Williams, F. Royo, O. Aizpurua-Olaizola, R. Pazos, G.-J. Boons, N.-C. Reichardt and J. M. Falcon-Perez, *J. Extracell. Vesicles*, 2018, **7**, 1.
4 M. Mathieu, L. Martin-Jaular, G. Lavieu and C. Théry, *Nat. Cell Biol.*, 2019, **21**, 9–17.
5 V. Agrahari, V. Agrahari, P. A. Burnouf, C. H. Chew and T. Burnouf, *Trends Biotechnol.*, 2019, **37**, 707–729.
6 W. Liao, Y. Du, C. Zhang, F. Pan, Y. Yao, T. Zhang and Q. Peng, *Acta Biomater.*, 2019, **86**, 1–14.
7 X. Zhang, H. Zhang, J. Gu, J. Zhang, H. Shi, H. Qian, D. Wang, W. Xu, J. Pan and H. A. Santos, *Adv. Mater.*, 2021, **33**, 2005709.
8 Y. L. Liu, D. Chen, P. Shang, D. C. Yin, Y. Teramura, K. N. Ekdahl, K. Fromell, B. Nilsson and K. Ishihara, *Langmuir*, 2020, **36**, 12088–12106.
9 L. Yu, R. Feng, L. Zhu, Q. Hao, J. Chu, Y. Gu, Y. Luo, Z. Zhang, G. Chen and H. Chen, *Sci. Adv.*, 2020, **6**(47), eabb6595.
10 K. S. Lim, D. Y. Lee, G. M. Valencia, Y. W. Won and D. A. Bull, *Biochem. Biophys. Res. Commun.*, 2017, **482**, 1042–1047.
11 J. Leong, Y. T. Hong, Y. F. Wu, E. Ko, S. Dvoretskiy, J. Y. Teo, B. S. Kim, K. Kim, H. Jeon, M. Boppart, Y. Y. Yang and H. Kong, *ACS Nano*, 2020, **14**, 5298–5313.
12 J. Park, B. Andrade, Y. Seo, M. J. Kim, S. C. Zimmerman and H. Kong, *Chem. Rev.*, 2018, **118**, 1664–1690.
13 S. Abbina, E. M. J. Siren, H. Moon and J. N. Kizhakkedathu, *ACS Biomater. Sci. Eng.*, 2018, **4**, 3658–3677.
14 Y. L. Liu, D. Chen, P. Shang and D. C. Yin, *J. Controlled Release*, 2019, **302**, 90–104.
15 X. Tang, F. Jing, B. Lin, S. Cui, R. Yu, X. Shen and T. Wang, *ACS Appl. Mater. Interfaces*, 2018, **10**, 15001–15011.
16 C. Yao, Y. Yuan and D. Yang, *ACS Appl. Bio Mater.*, 2018, **1**, 2012–2020.
17 R. Kawasaki, Y. Sasaki, K. Katagiri, S. Mukai, S. Sawada and K. Akiyoshi, *Angew. Chem., Int. Ed.*, 2016, **55**, 11377–11381.
18 Z. Zhuo, J. Wang, Y. Luo, R. Zeng, C. Zhang, W. Zhou, K. Guo, H. Wu, W. Sha and H. Chen, *Acta Biomater.*, 2021, **134**, 13–31.
19 C. M. Csizmar, J. R. Petersburg and C. R. Wagner, *Cell Chem. Biol.*, 2018, **25**, 931–940.
20 P. Shi and Y. Wang, *Angew. Chem., Int. Ed.*, 2021, **60**(21), 11580–11591.
21 M. You, Y. Lyu, D. Han, L. Qiu, Q. Liu, T. Chen, C. Sam Wu, L. Peng, L. Zhang, G. Bao and W. Tan, *Nat. Nanotechnol.*, 2017, **12**, 453–459.
22 D. C. Church and J. K. Pokorski, *Angew. Chem., Int. Ed.*, 2020, **59**, 11379–11383.
23 D. Takahashi, Y. Koda, Y. Sasaki and K. Akiyoshi, *Polym. J.*, 2018, **50**, 787–797.
24 J. Liu, Z. Ye, M. Xiang, B. Chang, J. Cui, T. Ji, L. Zhao, Q. Li, Y. Deng, L. Xu, G. Wang, L. Wang and Z. Wang, *Biomaterials*, 2019, **223**, 119475.
25 H. Cheng, J. H. Fan, L. P. Zhao, G. L. Fan, R. R. Zheng, X. Z. Qiu, X. Y. Yu, S. Y. Li and X. Z. Zhang, *Biomaterials*, 2019, **211**, 14–24.
26 L. Liu, H. He and J. Liu, *Polymers*, 2019, **11**, 2017.
27 S. I. Sawada, Y. T. Sato, R. Kawasaki, J. I. Yasuoka, R. Mizuta, Y. Sasaki and K. Akiyoshi, *Biomater. Sci.*, 2020, **8**, 619–630.
28 R. Mizuta, Y. Sasaki, R. Kawasaki, K. Katagiri, S.-I. Sawada, S.-A. Mukai and K. Akiyoshi, *Bioconjugate Chem.*, 2019, **30**(8), 2150–2155.
29 T. Ueda, S. J. Lee, Y. Nakatani, G. Ourisson and J. Sunamoto, *Chem. Lett.*, 1998, **27**, 417–418.
30 Y. Sekine, Y. Moritani, T. Ikeda-Fukazawa, Y. Sasaki and K. Akiyoshi, *Adv. Healthcare Mater.*, 2012, **1**, 722–728.
31 M. Alavi, N. Karimi and M. Safaei, *Adv. Pharm. Bull.*, 2017, **7**, 3–9.

32 R. Nisini, N. Poerio, S. Mariotti, F. De Santis and M. Fraziano, *Front. Immunol.*, 2018, **9**, 1.
33 E. Yuba, *J. Mater. Chem. B*, 2020, **8**, 1093–1107.
34 D. Chatzikleanthous, S. T. Schmidt, G. Buffi, I. Paciello, R. Cunliffe, F. Carboni, M. R. Romano, D. T. O'Hagan, U. D'Oro, S. Woods, C. W. Roberts, Y. Perrie and R. Adamo, *J. Controlled Release*, 2020, **323**, 125–137.
35 Y. Wei, S. Song, N. Duan, F. Wang, Y. Wang, Y. Yang, C. Peng, J. Li, D. Nie, X. Zhang, S. Guo, C. Zhu, M. Yu and Y. Gan, *Adv. Sci.*, 2020, 1902746.
36 K. Katagiri, K. Ohta, K. Sako, K. Inumaru, K. Hayashi, Y. Sasaki and K. Akiyoshi, *Chempluschem*, 2014, **79**, 1631–1637.
37 A. Görgens, M. Bremer, R. Ferrer-Tur, F. Murke, T. Tertel, P. A. Horn, S. Thalmann, J. A. Welsh, C. Probst, C. Guerin, C. M. Boulanger, J. C. Jones, H. Hanenberg, U. Erdbrügger, J. Lannigan, F. L. Ricklefs, S. El-Andaloussi and B. Giebel, *J. Extracell. Vesicles*, 2019, **8**, 1587567.
38 F. L. Ricklefs, C. L. Maire, R. Reimer, L. Dührsen, K. Kolbe, M. Holz, E. Schneider, A. Rissiek, A. Babayan, C. Hille, K. Pantel, S. Krasemann, M. Glatzel, D. H. Heiland, J. Flitsch, T. Martens, N. O. Schmidt, S. Peine, X. O. Breakefield, S. Lawler, E. A. Chiocca, B. Fehse, B. Giebel, A. Görgens, M. Westphal and K. Lamszus, *J. Extracell. Vesicles*, 2019, **8**, 1588555.
39 S. Mastoridis, G. M. Bertolino, G. Whitehouse, F. Dazzi, A. Sanchez-Fueyo and M. Martinez-Llordella, *Front. Immunol.*, 2018, **9**, 1583.
40 R. Kawasaki, Y. Sasaki, T. Nishimura, K. Katagiri, K. Morita, Y. Sekine, S. Sawada, S. Mukai and K. Akiyoshi, *Adv. Healthcare Mater.*, 2021, 2001988.
41 R. J. Malcolmson, J. Higinbotham, P. H. Beswick, P. O. Privat and L. Saunier, *J. Membr. Sci.*, 1997, **123**, 243–253.
42 T. Skotland, K. Sagini, K. Sandvig and A. Llorente, *Adv. Drug Delivery Rev.*, 2020, **159**, 308–321.